Turkish Journal of Engineering & Environmental Sciences

http://journals.tubitak.gov.tr/engineering/

Research Article

Turkish J Eng Env Sci
(2014) 38: 392 – 403

doi:10.3906/muh-1404-2

Experimental assessment of changes of sandy beach profile and sediment transport caused by tsunami waves

Mohammad DALIRI*, **Amir Houshang NEZAMIVAND CHEGINI**
Faculty of Engineering, University of Guilan, Main Campus, Rasht, Guilan, Iran

Received: 08.04.2014 • **Accepted/Published Online:** 07.10.2015 • **Printed:** 04.03.2016

Abstract: Destructive solitary (tsunami) waves are capable of moving large amounts of coastal sediments and causing subsequent morphological changes in sandy beaches. Experimental studies can be significantly helpful to assess the process of sediment transport brought about by a tsunami. The present study is an experimental one that aims to investigate sediment transport and deformation of sandy beaches caused by tsunami waves. Waves were generated by a gate wave-producing system to simulate tsunami waves. Laboratory equipment and mounted cameras were applied to examine run-up and run-down processes of waves and the beach profile changes were drawn. The techniques of estimating the transport rate of sediment particles is based on the four traps set in different parts of the beach. The obtained results showed that waves were not capable of transporting the sediment in regions far from the coast where shoaling effects were not considerable. Furthermore, wave breaking point and its distance from each trap have significant effects on the sediment transport assessment of that region. Moreover, the achieved findings indicate that sediment transport that occurred in the run-down of the waves was more effective than that from run-up.

Key words: Tsunami waves, changes of sandy beach profile, sediment transport, solitary waves

1. Introduction

Tsunamis are sea-surface gravity waves caused by the displacement of large volumes of water body, which are triggered by underwater earthquakes, volcanic eruptions, large-scale coastal landslides, meteorite collisions, and underwater nuclear explosions. Sediment transport brings about severe damage to human beings, constructions, coastal topography, and environmental processes. Scour and erosion resulting from a tsunami can cause serious damage to construction infrastructures, roads, highways, underground pipelines, coastal embankments, or other shoreline structures. Due to their long periods, tsunamis are often modeled as solitary waves in physical and theoretical studies. In comparison to a lot of research conducted in the field of morphological changes due to currents or regular waves, few experimental studies were accomplished in association with erosion and sedimentation patterns caused by a tsunami. Kobayashi and Lawrence [1] did laboratory experiments to examine the cross-shore sediment transport processes under breaking solitary waves on a fine sand beach. The initial beach slope of 1/12 was exposed to a positive solitary wave eight times and then the beach was rebuilt and exposed to a negative solitary wave eight times. Moronkeji [2] studied the effects of solitary and cnoidal waves on a sandy beach with four different slope conditions to investigate sediment transport and morphological changes. Solitary wave heights of 10, 30, 50, and 60 cm and cnoidal waves of 30 and 50 cm were tested with respective wave lengths of 12 and 8 m. Tsujimoto et al. [3] examined the beach profile changes under solitary waves alone

*Correspondence: moh.daliri@gmail.com

and in combination with regular waves. Young et al. [4] investigated the erosion and deposition patterns under breaking positive solitary waves. They found that tsunami run-up and run-down can cause liquefaction failure of coastal fine sand slopes due to the generation of high excess pore pressure and the reduction of the effective overburden pressure during the run-down. On the other hand, tsunami-induced sediment transport has been studied by several authors using various numerical models such as Apotsos et al. [5], Goto and Imamura [6], Li et al. [7], Nakamura et al. [8], Simpson and Castelltort [9], Sugawara et al. [10], Takahashi et al. [11], and Xiao et al. [12]. Although much research has been conducted related to sediment transport, various mechanisms of this process are still unknown, which could be rooted in the hydrodynamic conditions of waves and geology. For example, the stochastic nature of sediment particle movement, determination of the transition zone between bed load or suspended load, and inadequate compliance laboratory models with field observation are problems that should be assessed more accurately.

2. Theoretical approach

Tsunamis behave like long waves on shallow water due to their long wave lengths, even if they occur in deep waters. In one dimension, the classic equations used for nonlinear long waves can be defined by the following:

$$\frac{\partial \eta}{\partial t} + \frac{\partial[(h+\eta)u]}{\partial x} = 0,$$

$$\frac{\partial u}{\partial t} + u\frac{\partial u}{\partial x} + g\frac{\partial \eta}{\partial x} = 0,$$

where h stands for water depth, η for wave amplitude, u for the depth averaged velocity, t for time, and g for gravitational acceleration. Carrier and Greenspan [13], Keller and Keller [14], and Synolakis [15] proposed some analytical solutions for the above equations. Finally, using a solitary wave, the following equations were suggested for evaluating the water surface:

$$\eta = H \sec h^2 \sqrt{\frac{3H}{4h^3}}(x - ct),$$

$$c = \sqrt{g(H+h)},$$

$$u = \eta\sqrt{\frac{g}{h}},$$

in which H refers to water height and c refers to wave celerity. Xiao et al. [12] used a mathematical model that joined water flow dynamics and sediment transport. This model is capable of assessing morphological changes of the affected solitary waves. Suggested formulas in this section are structured based on the shallow-water theory, which assumes that the vertical component of acceleration has a negligible effect on the fluid pressure (i.e. pressure is hydrostatic). For the flow over a moveable bed, the shallow-water equations are coupled to equations for the conservation of sediment mass, momentum, and bed topography:

$$\frac{\partial h}{\partial t} + \frac{\partial (hu)}{\partial x} = \frac{q_e - q_d}{1-\varphi},$$

$$\frac{\partial (hu)}{\partial t} + \frac{\partial (hu^2 + \frac{1}{2}gh^2)}{\partial x} = -gh(s - s_f) - \frac{(q_e - q_d)u}{1-\varphi},$$

$$\frac{\partial(hC)}{\partial t} + \frac{\partial(huC)}{\partial x} = q_e - q_d,$$

$$\frac{dz}{dx} = \frac{q_d - q_e}{1 - \varphi},$$

where C represents depth-averaged sediment concentration, s_f represents bottom friction slope, s refers to bed slope where z is the bed surface elevation, φ is bottom sediment porosity, and q_e and q_d refer to substrate entrainment and deposition fluxes across the bottom boundary of flow (representing sediment exchange between the water column and bed). Making a balance between an erosive bed and flow can bring about two different mechanisms. The first is the erosion of bottom sediment, due to severe turbulences of the flow, and the second is the sediment deposition resulting from the earth's gravitational operations. Determining erosion and deposition fluxes is considered a pivotal component of computational models for sediment transport and morphological deformations.

3. Experimental setup

All experiments were done in a glass side-wall wave flume located in the hydraulics laboratory of the Technical Faculty of Guilan University. The wave flume was 12 m long, 0.5 m wide, and 0.5 m high. A gate was applied at one end of the flume in order to produce the waves, in such a way that the water depth upstream was more than that downstream and the gate was suddenly opened to simulate conditions of tsunami (solitary) waves. Depending on the water level difference behind and in front of the gate, bore or solitary waves can be produced. The bore is generated when the water level difference behind and in front of the gate is high and meanwhile the downstream level is very low. Goto and Imamura [6] used this system of bore generation for their experiments. On the other hand, when the water level difference behind and in front of the gate is not too high and the downstream level is not low, a solitary wave can be generated. Esteban et al. [16] generated solitary waves using this method for assessment of pressure exerted by a solitary wave on the rubble mound foundation of an armored caisson breakwater. All waves generated in this study were solitary waves, which are among the most appropriate waves to simulate tsunami waves. Three ultrasonic wave gauges were used to measure wave surface elevations by a 6-channel data logger, in which three sensors were active, responsible for receiving the signals. Two adjustable rulers (measurements) were mounted before and after the gate in order to control the upstream and downstream water level in each test. Figure 1 provides an image of the flume, measurement tools, and wave-producing system. Figure 2 shows a typical solitary wave generated using the aforementioned system in the wave flume.

A sand beach with a slope of 1/13.8 and mean grain diameter $D_{50} = 0.2$ mm was constructed at the downstream end of the wave flume so that its toe was located 530 cm away from the gate. The specific gravity of particles was 2.66 g/cm^3 and thickness of the sand on beach was 3 cm.

Wave motion in the flume and its breaking caused turbulence and sediment transport. Transported sediment was examined by the traps installed along the beach slope. These traps were utilized to capture transported sediments during wave run-up or run-down. Three traps with length of 48 cm, width of 15 cm, and adjustable height of 2 to 4 cm (depending on beach thickness) and a fourth trap with length of 85 cm, width of 48 cm, and adjustable height of 2 to 4 cm were built to collect sediment particles. Figure 3 shows an image of the sandy beach and its traps.

Figure 1. A view of the flume, measurement tools, and wave-producing system.

Figure 2. Typical solitary wave created in the wave flume.

Figure 3. Sandy beach and its traps.

4. The process of wave breaking and bed morphological results

Experiments were done to assess the deformation of sandy beach profile. Figure 4a indicates temporal changes in the solitary wave profile generated by the wave-producing system, considering the downstream depth of 14 cm and upstream depth of 30 cm. Sensor 1 was installed at a distance of 0.5 m before the toe of the slope in order to recognize the incoming waves, and sensors 2 and 3 were set at distances of 0.7 and 1.7 m after the toe of the slope in order to recognize the shoaling and breaking.

Height of the generated waves was calculated as about 10 cm (regarding sensor 1) and about 11 to 11.5 cm (regarding sensor 2). Figure 4b makes a comparison between the solitary wave profile derived from Eq. (3) and the measured wave profile using sensor 1. The exact recorded water depth and wave height were 140 mm and 102.96 mm, respectively, and these values were used in Eq. (3). As shown in Figure 4b, the measured wave profile has a reasonable compliance with the theoretical wave profile. However, the measured wave profile is followed by oscillatory waves that are not seen in the theoretical wave profile. This discrepancy refers to the wave-producing system used this study.

Observations from recorded videos showed that the waves were broken at a short distance just after sensor 2 and reduction of wave height at sensor 3 indicates a breaking phenomenon (Figure 5a). Grilli et al.

[17] defined the dimensionless slope parameter S_0 for solitary waves as a breaking criterion as follows:

$$S_0 = 1.521 \frac{s}{\sqrt{H/h}},$$

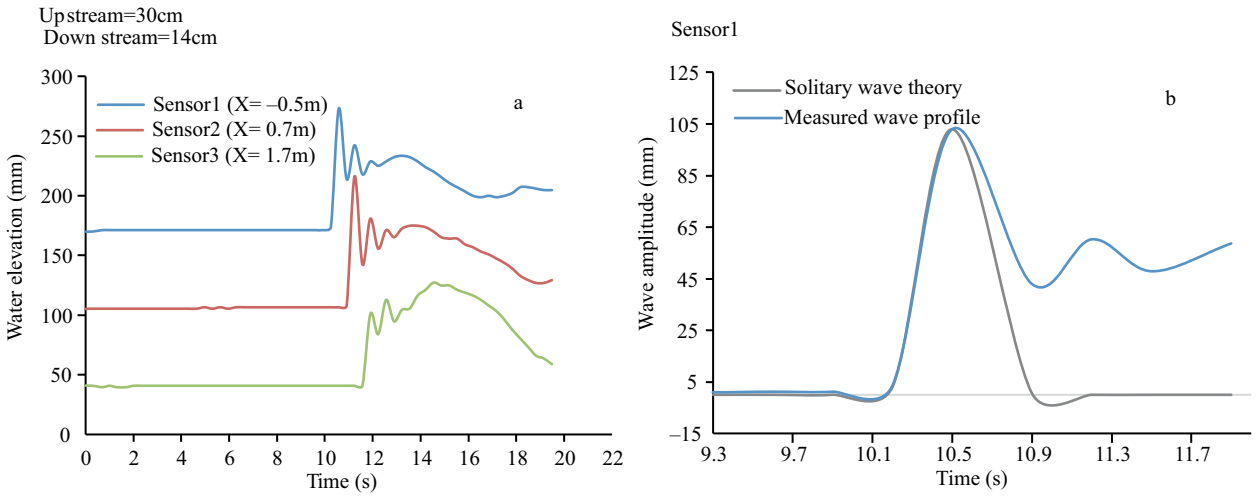

Figure 4. Temporal variation of the measured solitary wave profile (a) at different sensors and (b) with the theoretical profile.

where s is beach slope and H/h is dimensionless wave height. With slope parameter it can be predicted whether a solitary wave will break or not and which type of breaking will occur. Their experiments showed that waves will break when $S_0 < 0.37$ and the type of breaking can be classified as follows:

Surging breaking: $0.3 < S_0 < 0.37$,

Plunging breaking: $0.025 < S_0 < 0.3$,

Spilling breaking: $S_0 < 0.025$.

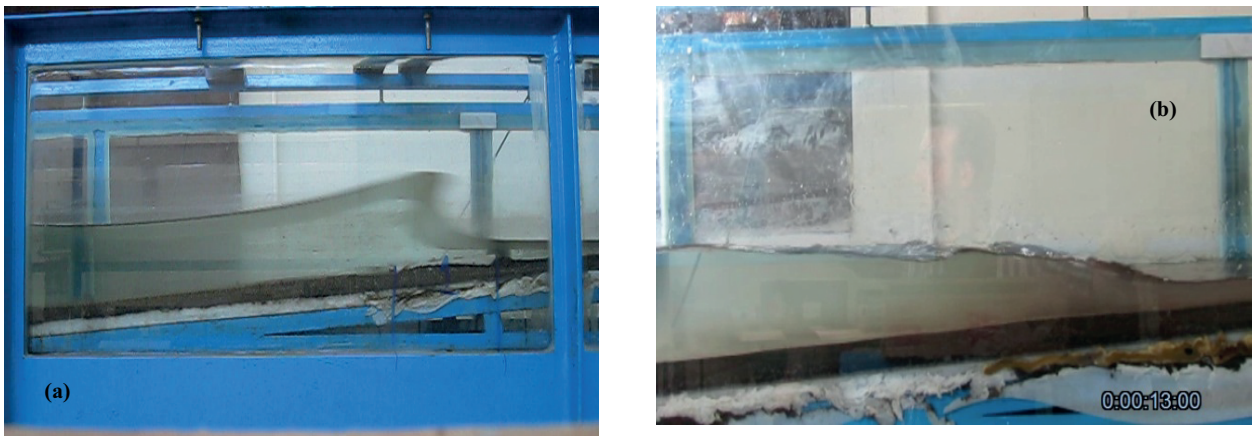

Figure 5. Typical photos of flow pattern: (a) instant of wave breaking and (b) hydraulic jump observed in the flume.

These results were confirmed through computational and experimental works. All generated waves in this study were broken and classified as the plunging type. In order to assess the wave celerity, the distance between adjoined gauges (sensors 1 and 2) was divided by the travel time between these sensors ($c = 1.7$ m/s).

The velocity of a solitary wave, based on Eq. (5), was calculated as about 1.53 m/s, which is consistent with the experimental results. The discrepancy between these values arises from the wave-producing system, which generates a solitary wave that does not fully match the theoretical one.

Considering the peculiarities of the coastline and objective observations, the highest rising level of SWL was 17 cm. Experimental studies of Fuhrman and Madsen [18] brought about the following formula for solitary wave run-up:

$$\frac{R}{H} = 3.9\xi_S^{0.42} \quad , \quad \xi_S = \frac{s}{H/h} \quad ,$$

where R refers to run-up and ξ_S is the surf similarity parameter for a solitary wave. According to this formula run-up is 15 cm, which is compatible with the experimental results (17 cm). The wave breaks on a thin layer of water before reaching the coastline. In order to obtain a better accuracy in the measurement of the bed profile, the bed was subjected to two solitary waves at an interval of 15 min. Observing the recorded videos, it can be seen that sediment concentration does not enhance suddenly after the wave breaks. This is due to the breaking wave on the thin layer of water before reaching the coastline. Then a bore is constructed, which suspends a large volume of sand from the bed and moves forwards due to the water momentum. At the maximum run-up height, water depth is considerably low, sediment concentration is high, and flow velocity is about zero. All these conditions cause sediment deposition in the water. The run-down process consists of a strong sediment concentration sheet flow and a rotational region of the flow similar to hydraulic jump. When the wave reaches the highest level, it starts to return towards the sea. While returning, the incident wave faces a large amount of return water depth and a similar hydraulic jump occurs. A considerable amount of sediment is also transported while the wave returns back, as shown in Figure 5b. In this region, the velocity of returning flow and sediment concentration are high while water depth is low, which causes an erosion region. When water with high concentration enters the rotational flow of the hydraulic jump, the velocity of the flow suddenly decreases and sediments enter the rotational flow of the hydraulic jump; thus, they are deposited around the wave breaking point.

Figure 6 demonstrates a schematic vision of erosion, deposition, and sediment transport regions. Ripples, caused by returning flow, hydraulic jump, and turbulence in deposition regions, are perfectly observed. In this experiment, bed profile variations were calculated in four different paths and sand thickness was totally measured at 156 points using a point gauge. Figure 7 demonstrates the beach profile affected by two solitary waves at an interval of 15 min.

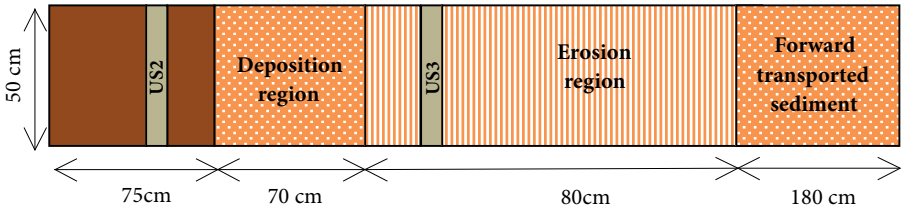

Figure 6. Schematic vision of the erosion, deposition, and sediment regions.

5. Results of sediment transport

In the last part of the study, deformation of a sandy beach under tsunami waves was investigated. This section deals with the amount of transported sediment at different points or times. Four traps were used to measure the amount of sediment transport. Trap 1 was installed at the toe of the beach; traps 2 and 3 were set at distances of 120 and 240 cm from the toe respectively and trap 4 was set at the end of the beach. These traps were

utilized to assess the amount of sediment transport caused by a series of 5 solitary waves of various heights. The experiments were conducted at upstream water depths of 30, 31, 32, 33, and 34 cm and downstream levels of 14, 15, 16, 17, and 18 cm. Related data to each wave series are shown in the Table. Figure 8 indicates the flume, sensors, traps, and cameras in test 1. In this figure, TR stands for trap, US stands for ultrasonic sensor, and CA stands for camera.

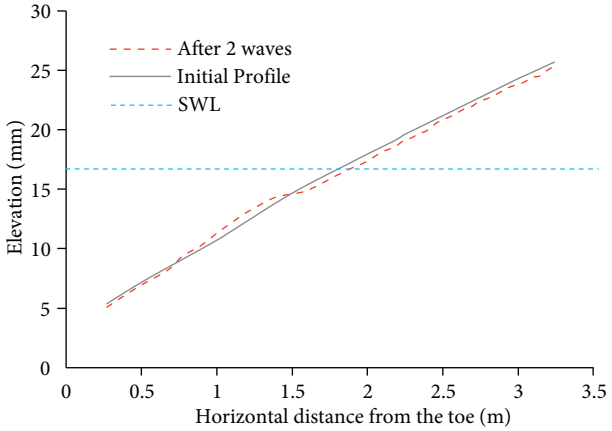

Figure 7. Deformation of sandy beach affected by two solitary waves.

Table. Parameters of the waves generated for sediment transport measurements.

Test number	Downstream depth (cm)	Upstream depth (cm)	Breaking point from the toe (cm)	Classification
1	14	30	120	Plunging
2	15	31	135	Plunging
3	16	32	150	Plunging
4	17	33	170	Plunging
5	18	34	190	Plunging

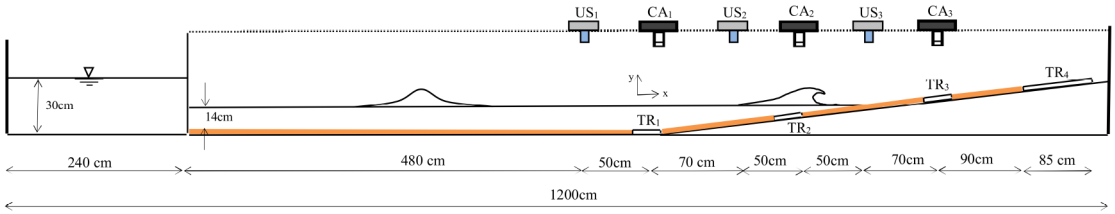

Figure 8. Schematic cross-sectional diagram of the flume, sensors, traps, and cameras.

As it has been mentioned, incident waves are considerably effective in sediment transport while rushing up and down the beach. In the current study, all waves broke between traps 2 and 3 and the height of incident waves was calculated at around 10 to 11 cm. When a wave is moving forward, some sediments are transported to the traps before rushing down, which are called 'forward sediments'. When the wave reaches the highest level on the coastline, it starts returning and transports and deposits a huge amount of sediments to the traps; these sediments are called 'backward sediments'. Having completed each experiment, water inside the flume was drained and sediments were collected and weighed after drying. These sediments were the sum of forward and backward sediments. Owing to the fact that intervals between run-up and run-down of the waves were short and there was not enough time to collect and evaluate the forward sediments, recorded videos were processed to

estimate forward sediment weight. Three cameras were mounted at the top of traps TR1, TR2, and TR3 in order to record what happened in each trap while waves were running up and down. When reviewing the recorded films, a photo was taken at the moment that the incident wave had completely passed the trap and water above the trap became stationary. Using this photo, the amount of trapped forward sediment was estimated. Backward sediment was estimated by subtracting the total weight of sediment from forward sediment.

Experimental observations indicated that none of the waves could transport significant amounts of sediment to trap 1. Since trap 1 was set at the beach toe, incident waves at this point had more depth in proportion to waves near the breaking region. Thus, they were less effective in the bed and could not transport much sediment. Volume of transported sediment (V_S) depends on many factors such as wave height (H), water depth (h), beach slope (s), sand diameter (D), water density (γ_w), sand density (γ_s), distance between the toe of the beach and the breaking point (X_b), and gravitational acceleration (g). Since the assessment of all aforementioned factors is not possible in a single article, a dimensional analysis approach has been applied. The Buckingham π theorem was used for computing sets of dimensionless parameters from the given variables:

$$f(V_S, H, h, s, D, \gamma_w, \gamma_s, X_b, g) = 0,$$

$$\pi_1 = \frac{V_S}{H^2} \ , \quad \pi_2 = \frac{X_b}{H} \ , \quad \pi_3 = \frac{h}{H} \quad , \quad \pi_4 = \frac{D}{H} \quad , \quad \pi_5 = \cot s \ , \quad \pi_6 = \frac{\gamma_s}{\gamma_w} = G_s,$$

where G_s represents the speci?c gravity of sand. The dimensionless parameter of transported sediment volume in width (π_1) can be considered as a function of five other dimensionless parameters:

$$\frac{V_S}{H^2} = F(\frac{DG_sX_b}{hH}\cot s).$$

In order to obtain the function F, (V_S/H^2) should be calculated using laboratory data and based on the dimensionless parameter of $(DG_sX_b \cot s/hH)$; a logical relationship should also be established between them. The dimensionless parameter of $(DG_sX_b \cot s/hH)$ is shown as a new parameter λ, which is directly associated with wave breaking point (X_b), while it is negatively related to water depth (h). Due to the fact that change in water depth is small compared to change in the location of the wave's breaking point, it can be concluded that parameter λ increases with increasing wave breaking point. Notice that other factors affecting parameter λ are approximately fixed in this experiment. Figures 9a and 9b show variations of the trapped sediments' weight and related transported sediments' volume in width (V_s/H^2) against parameter λ during the forward and backward motion in trap 2, respectively. Two important points can be understood from these figures. First, in all tests (except test 5) the backward sediments were considerably more than forward sediments, and the second point is that by increasing parameter λ, the backward sediments decreased in such a way that the proportion of backward sediments in the fifth and third tests to the first test decreased by 95% and 63% respectively while there was not a considerable change in forward sediments. Consequently, the total amount of sediment transported to trap 2 decreased. Since almost all waves break after trap 2, increasing λ cannot significantly change forward sediments and decreases backward sediments. This could be the result of increasing distance from the hydraulic jump when run down from trap 2. As was mentioned in Section 4, water flow experiences a hydraulic jump near the breaking point when running down, which strongly decreases sheet flow velocity and subsequently sediment deposit. For the waves that break far from trap 2, sediment is deposited farther away, and an increase in parameter λ yields a decrease in the width of the transported sediment volume when moving backward.

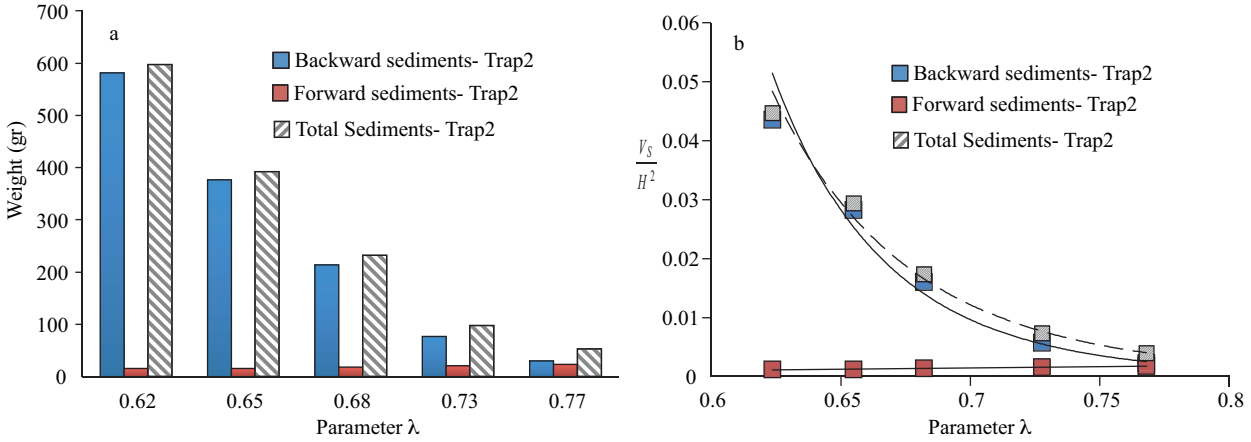

Figure 9. Variation of parameter λ during forward and backward motion at trap 2 with the transported (a) sediment weight and (b) sediment volume (V_s/H^2).

Figures 10a and 10b show variations of the trapped sediments' weight and related transported sediments' volume in width (V_s/H^2) against parameter λ during the forward and backward motion in trap 3, respectively. All waves had broken before reaching this trap, and, like trap 2, in all tests the backward sediments were more than forward sediments. For trap 3, however, an increase in λ resulted in a 73% increase in the amount of backward sediments and a 60% decrease in the amount of forward sediments when the fifth test was compared to the first test. As can be seen in the figures, these increases and decreases are linear so the total amounts of trapped sediments in each test in trap 3 are not changed significantly.

It can be observed that the increase of parameter λ decreases the transported sediment volume in width in trap 3 when moving forward. In previous sections it was mentioned that a wave cannot transport significant amounts of sediment immediately after breaking. The waves that break near trap 3 are thus less capable of transporting sediments. Figure 10b also indicates the sediment volume transported to trap 3 when moving backward. The farther a wave breaks from trap 3, the farther the sediment is deposited after the hydraulic jump when moving backward. Thus, the waves that break closer to trap 3 can transport more amounts of sediment to this trap when moving backward. Furthermore, backward sediments are more in quantity than forward sediments.

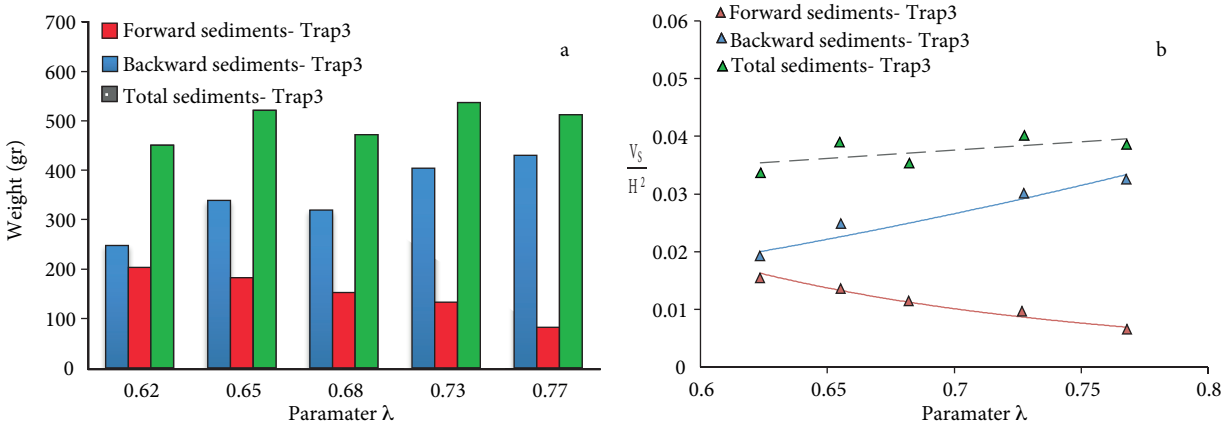

Figure 10. Variation of parameter λ during forward and backward motion at trap 3 with the transported (a) sediment weight and (b) sediment volume (V_s/H^2).

Figures 11a and 11b show variations of the total trapped sediments' weight and related transported sediments' volume in width (V_s/H^2) against parameter λ in traps 2, 3, and 4. It can be seen that by increasing λ the total sediments in trap 4 increase in such a way that the amount of sediments in the fifth test increases by 130% compared to the first test. On the other hand, as mentioned before, the total amount of sediments in trap 2 decreases and there is no significant change in the total amount of sediment in trap 3. Since trap 4 is located at the end of the beach and far from the breaking point, the broken waves should travel a long path in order to transport the sediment. If the wave breaks far from trap 4, it loses its energy to transport the sediment, while the waves that break closer to trap 4 can transport more sediment. Thus, the increase of parameter λ can enhance transported sediment volume in width.

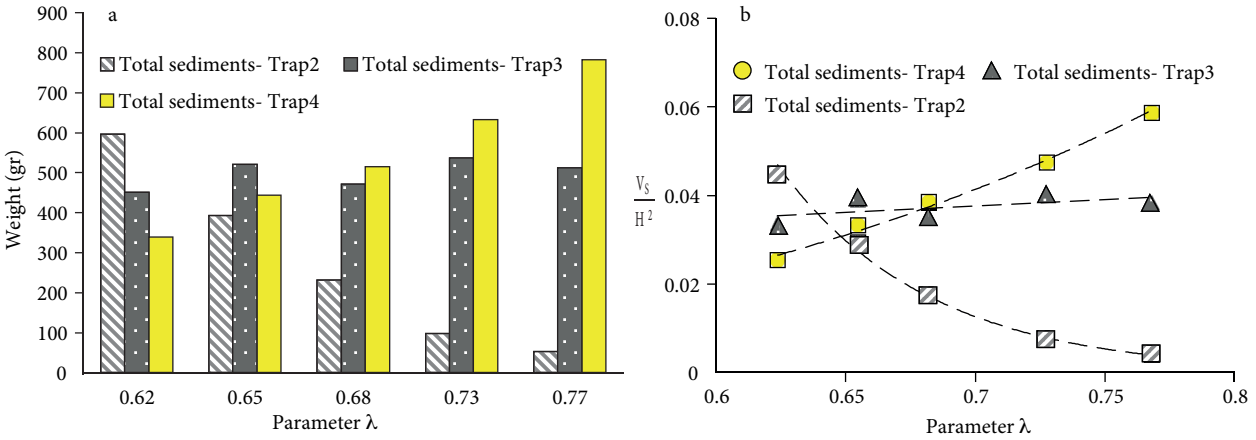

Figure 11. Comparison of parameter λ during forward and backward motion at all traps with the total transported (a) sediment weight and (b) sediment volume (V_s/H^2).

6. Conclusion

The current study was an experimental one that was conducted in the wave flume of Guilan University and aimed to investigate sediment transport and deformation of sandy beaches caused by tsunami (solitary) waves of various heights. The achieved findings showed that a solitary wave can transport sediment after breaking and move forward. When it moves backward, the transported sediments are moved towards the breaking point and deposited near it. The existing ripples caused by the returning wave, hydraulic jump, and turbulence in deposition regions were completely clear. Four traps were set in different parts of the beach to measure the sediment transport caused by incident solitary waves. The findings indicated that tsunami waves cannot transport much sediment in regions far from the beach due to the high water depth (like trap 1 in this experiment), while in nearer regions they are capable of transporting a large amount of sediment. All waves in this experiment were broken between traps 2 and 3 (Figure 8). In the regions beyond the breaking point (like trap 2 in Figure 8), the location of the breaking point does not bring about a considerable change in the amount of sediment transport when moving forward, while it decreases significantly when moving backward. Thus, the total transported sediments to these regions decrease. It should be noted that backward sediments were much greater in quantity than forward sediments. In the regions located near the breaking point and after that (like trap 3 in Figure 8), decreasing the distance from the breaking point could result in less forward sediment transport, and much sediment is transported when moving backward. Besides that, increases and decreases in the amount of the transported sediment are approximately equal, which results in a small amount

of the total transported sediment in this region. Furthermore, backward sediments were more in quantity than forward ones in this trap. In the regions far from the breaking point and after that (like trap 4 in Figure 8), decreasing the distance of wave breaking from the trap can enhance the sediment transport to the trap, since waves that break far from the trap lose their energy to transport sediment.

Nomenclature

h	water depth	TR	trap
η	wave amplitude	s	bed slope
u	depth averaged velocity	ξ_S	surf similarity parameter
t	time	R	run-up
H	water height	S_0	dimensionless slope parameter
c	wave celerity	D	sand diameter
C	depth-averaged sediment concentration	γ_s	water density
q_e	substrate entrainment flux	γ_s	sand density
q_d	deposition flux	G_s	specific gravity of sand
φ	bottom sediment porosity	X_b	distance from the toe to the breaking point
s_f	bottom friction slope	V_S	transported sediment volume
CA	camera	λ	dimensionless parameter
		US	ultrasonic sensor

References

[1] Kobayashi N, Lawrence A. Cross shore sediment transport under breaking solitary waves. J Geophys Res 2004; 109: 13.

[2] Moronkeji A. Physical modelling of tsunami induced sediment transport and scour. In: Proceedings of the 2007 Earthquake Engineering Symposium for Young Researchers; 8–12 August 2007; Seattle, WA, USA.

[3] Tsujimoto G, Yamada F, Kakinoki T. Time-space variation and spectral evolution of sandy beach profiles under tsunami and regular waves. In: Proceedings of the 18th International Offshore and Polar Engineering Conference, Vol. 3. Vancouver, Canada: ISOPE; 2008. pp. 523–527.

[4] Young YL, Xiao H, Maddux T. Hydro-and morpho-dynamic modeling of breaking solitary waves over a fine sand beach. Part I: Experimental study. Mar Geol 2010; 269: 107–118.

[5] Apotsos A, Gelfenbaum G, Jaffe B. Process-based modeling of tsunami inundation and sediment transport. J Geophys Res 2011; 116: 20.

[6] Goto K, Imamura F. Numerical models for sediment transport by tsunamis. Quaternary Res 2007; 46: 463–475.

[7] Li LL, Huang ZH, Qiu Q, Natawidjaja DH, Sieh K. Tsunami-induced coastal change: scenario studies for Painan, West Sumatra, Indonesia. Earth Planets Space 2012; 64: 1–18.

[8] Nakamura T, Mizutani N, Yim SC. A three-dimensional coupled fluid-sediment interaction model with bed-load/suspended-load transport for scour analysis around a fixed structure. J Offshore Mech Arct Eng 2009; 131: 1–9.

[9] Simpson G, Castelltort S. Coupled model of surface water flow, sediment transport and morphological evolution. Comput Geosci 2006; 32: 1600–1614.

[10] Sugawara M, Ohkubo S, Imamura F. Basic study on sand sedimentation by a tsunami on an uniform slope. Tohoku Journal of Natural Disaster Science 2004; 40: 265–270.

[11] Takahashi T, Shuto N, Imamura F, Asai D. Modeling sediment transport due to tsunamis with exchange rate between bed load layer and suspended load layer. In: Proceedings of the 27th International Conference on Coastal Engineering, Vol. 2. Sydney, Australia: ASCE; 2000. pp. 1508–1519.

[12] Xiao H, Young YL, Prevost JH. Hydro- and morpho-dynamic modeling of breaking solitary waves over a fine sand beach. Part II: Numerical simulation. Mar Geol 2010; 269: 119–131.

[13] Carrier G, Greenspan H. Water waves of finite amplitude on a sloping beach. J Fluid Mech 1958; 4: 97–109.

[14] Keller JB, Keller HB. Water Wave Run-Up on a Beach. ONR Research Report. Contract NONR-3828(00). Washington, DC, USA: Department of the Navy, 1964.

[15] Synolakis CE. The run-up of solitary waves. J Fluid Mech 1987; 185: 523–545.

[16] Esteban M, Danh Thao N, Takagi H, Shibayama T. Pressure exerted by a solitary wave on the rubble mound foundation of an armoured caisson breakwater. In: 19th International Offshore and Polar Engineering Conference, Vol. 3. Osaka, Japan: ISOPE, 2009. pp. 1137–1144.

[17] Grilli ST, Svendsen IA, Subramanya R. Breaking criterion and characteristics for solitary waves on slopes. J Waterw Port Coastal Ocean Eng 1997; 123: 102–112.

[18] Fuhrman DR, Madsen PA. Surf similarity and solitary wave run-up. J Waterw Port Coastal Ocean Eng 2008; 134: 195–198.